Powder Technology 415 (2023) 118158

Contents lists available at ScienceDirect

Powder Technology

journal homepage: www.journals.elsevier.com/powder-technology

Novel contact force measurement in vibratory finishing

Shuwen Wang [a,*], Jiahui Chen [a], Zhiguo Liu [a], Michael Morgan [b], Xiaoxiao Liu [b]

[a] College of Mechanical Engineering, University of Shanghai for Science and Technology, Shanghai 200093, China
[b] General Engineering Research Institute, Liverpool John Moores University, Byrom Street, Liverpool L3 3AF, UK

HIGHLIGHTS

- A novel triaxial wireless force sensor is successfully developed.
- The VSFFs on different surfaces of a workpiece are measured.
- The efficiency of vibratory finishing on a workpiece has been investigated.

GRAPHICAL ABSTRACT

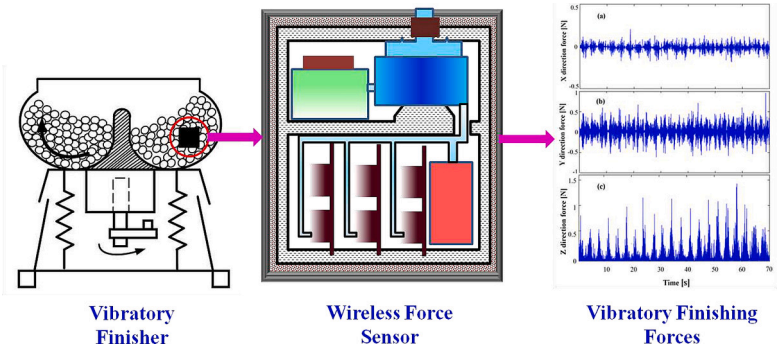

ARTICLE INFO

Keywords:
Vibratory surface finishing
Contact force
Wireless force sensor
Surface topography
Hardness

ABSTRACT

The measurement accuracy of vibratory surface finishing forces (VSFFs) are seriously affected by the wiring of the force sensor, because the trajectory of the sensor with wiring is significantly different with that of the workpiece without wiring. To solve this problem, a triaxial wireless force sensor (WFS) is developed to measure the VSFFs between media and workpiece surfaces in vibratory surface finishing under various operation conditions. Experimental results show that the normal impacts between the media and the workpiece are dominant in the vibratory surface finishing (VSF), and the mean VSFFs in normal direction on the front surface of the workpiece are larger than that on the side and rear surfaces of the workpiece. The mass and shape of media have a significant effect on the VSFFs that has significant effects on the surface roughness and hardness of a workpiece in the VSF. In order to get the best surface quality of workpiece in vibratory surface finishing, the media material and shape/size, finishing period of time, initial position of the workpiece, and other operation conditions should be optimized.

1. Introduction

The functional surfaces manufactured by machining or casting are normally have undesirable surface quality caused by burrs, scratches, or insufficient finish [1], which has significant effects on the performance and service life of functional surfaces and components. Therefore, many conventional and unconventional surface finishing or polishing processes have been used in manufacturing industry. The conventional

* Corresponding author.
E-mail address: kevinwang68@hotmail.com (S. Wang).

https://doi.org/10.1016/j.powtec.2022.118158
Received 3 October 2022; Received in revised form 17 November 2022; Accepted 8 December 2022
Available online 11 December 2022

surface polishing processes include manual polishing, grinding, chemical polishing, shot peening, abrasive polishing, and vibratory surface finishing [2,3]. The unconventional polishing processes include magnet abrasive finishing [4], ultrasonic-assisted magnetic abrasive finishing [5], low-plasticity burnishing [6], laser polishing [7,8], and deep ball-polishing [9].

Normally, the conventional surface polishing processes are convenient in operation, capable of dealing with large and complex components, and less cost. Compared with conventional surface polishing processes, the unconventional surface polishing processes have some limitations, such as the operations are complicated, difficult to polish large components with complex surfaces and holes, and expensive for large components. For example, Avilés [7] mentioned that, "Laser polishing is used to produce a relatively smooth surface finish in previously machined components. However, this process cannot achieve a perfectly smooth surface, and in many cases it cannot produce the degree of smoothness of a mirror finish. There are also some characteristic surface effects caused by this process, including surface pores, inclusions, and also micro-cracking, a consequence of the melting, evaporation and solidification stages".

Since the vibratory surface finishing (VSF) has strong adaptability, good processing quality, low economical cost, and no pollution in processing, it has been widely used for deburring, polishing, hardening, eliminating cracks, and improving wear resistance of functional surfaces and components for many decades [2,3].

In the VSF, the impact forces or vibratory surface finishing forces (VSFFs) between media particles and workpieces are critical to the effectiveness of this processing. In order to systematically study the mechanism of VSF, it is necessary to understand the interactions between the media and workpieces; however, it is very difficult to accurately measure the VSSFs, because the measurement accuracy of VSFFs between the surface finishing media and workpiece is significantly affected by the noise signals generated by the vibrations of the force sensor and its wiring.

Extensive research on VSF has been conducted by the researchers at the University of Toronto in Canada, the Nanyang Technological University in Singapore, the Aachen University in Germany, the Liverpool John Moores University in UK, and the Taiyuan University of Technology in China. In 2000, Wang et al. [3] first measured the normal contact forces of media in a vibratory finisher and compared these with the resulting changes in surface roughness and hardness of two aluminum alloys, AA-1100-O and AA-6061-T6. The principal variables were the media size, degree of lubrication and duration of the VSF. The changes in hardness and roughness of vibratory finished surfaces were found to depend mostly on the lubrication condition, the media roughness, and the size of the media, because these influenced the interactions between the media and the workpiece.

Based on the method proposed by Wang et al. [3], Yabuki et al. [10] measured both the normal and tangential contact forces between the media and a workpiece in the same bowl-type vibratory finishing machine. Together with a video system, it was established that actions between the finishing media and the test surface occurred in three different modes. The ratio of the normal and tangential forces was compared with the measured friction coefficient under dry and water-wet conditions, confirming that media sliding occurred more often under lubricated conditions.

Baghbanan et al. [11] used the same sensor employed in the study by Yabuki et al. [10] to measure the contact forces in a larger, more energetic tub finisher and to study their relation to the erosion and work hardening of aluminum. They found that the contact forces were generally greater in dry condition than that in wet condition when using water as a media lubricant.

Ciampini et al. [12] related the normal component of the measured contact forces in a vibratory finisher to the impact velocity using a piezo-electric transducer. This method provided a measure of the energy availability in the contacts that was independent of the sensor compliance. Consistent with Yabuki et al. [10], contacts could be classified as being either impact or non-impact events, depending on their duration. Both were expressed in terms of an 'effective' normal impact velocity. Although the piezo-electric sensor accurately measured the impact velocities, it was of interest to explore further the potential of the Almen system to provide a simpler characterization of the impact conditions in VSF.

Ciampini et al. [13] measured impact velocities within a granular bed using a stationary force sensor, and found that particle velocities were greater near the walls and increased with the increasing amplitude of tub vibration. Song et al. [14] also measured contact forces between media and work piece using a triaxial dynamometer, which was attached to a rigid wire. The sensor was mounted so that the contact forces could be measured in circumferential direction. Higher vibration frequencies and heavier media led to higher impact forces.

Lucas et al. [15] used a force sensor to measure the contact force between media and the wall of a vibratory finishing barrel and found that the wall contact force increased with the increasing of the media depth above the sensor and the normal wall velocity. Lachenmaier et al. [16] used two systems (workpiece with an integrated camera and workpiece with an integrated piezoelectric sensor) to measure the contact forces. The relative speed and the surface integrity of the processed workpiece were mainly affected by the speed and size of the grinding media. Ahluwalia et al. [17] proposed a dual vibratory finishing method, which used a vibratory fixture to make the processed workpiece reach saturation in a shorter time and employed a force sensor to study the rapid finishing mechanism.

Richard et al. [18] analyzed the influences of different factors, such as the size of media, the revolution acceleration of motor eccentric blocks, phase angle, and mass distribution, on finishing force. Wong et al. [19] combined statistical test results with a force sensor and asserted that the increased frequency resulted in a better polishing effect and significantly shortened the processing time.

Theoretical models also have been proposed to analyze the mechanical characteristics of barrel finishing. Hashimoto et al. [20] established a mechanical model of a vertical vibratory barrel polishing and finishing equipment to analyze the dynamic performance of the mechanical excitation system under free and forced vibrations. The impacts of the equipment was found to be the key factor to achieve better performance. Gaggar et al. [21] used a Lagrangian theoretical method based on the fluid dynamics of finishing media to simulate key indicators of the vibration polishing process.

Furthermore, the discrete element method (DEM) has been used to simulate VSFFs. Kang et al. [22] proposed a DEM-based vibrating machine model to study the three-dimensional motion of media in vibratory finishing. The model could calculate the normal and tangential finishing forces of media on workpiece surfaces. The influences of contact parameters, such as contact stiffness, friction, and damping, on the movement of media were also investigated. Yang et al. [23] selected the same experimental parameters used by Parker [24] for discrete element simulations, compared the simulation results with experimental findings, and used the finishing force of media and the relative collision speed and frequency between the media to verify the effectiveness of simulation results. Wang et al. [25] analyzed the vibratory finishing mechanism based on the contact force obtained by discrete element simulations and experiments, and provided guidance for actual vibratory finishing applications. Macie et al. [26] used DEM to predict the force exerted by the container wall on granular media and verified the predicted results with previous experimental measurements under different vibration frequencies and numbers of media. Hashemnia et al. [27] based on DEM, found that the impact velocity increased with the increasing of wall vibration amplitude, and the impact velocity of media was reduced at higher frequencies. Li et al. [28] conducted theoretical analysis and discrete element simulations to explore the influences of media movement and process parameters on centrifugal quality finishing. The force and speed of media in the finishing process were tested

and analyzed.

Moreover, Li et al. [29] developed a new type of polyurethane media with high strength, low elastic modulus, and good deformation adaptability. DEM was adopted to analyze the dynamic behavior of media with different mass ratios and hardness. It was found that as the hardness of media and the mass ratio of polyurethane raw rubber to abrasives increased, the velocity, energy, normal and tangential contact forces of the media increased.

The above studies have enhanced the experimental and theoretical understanding of VSF, especially barrel finishing force. However, owing to technological constraints, the influence of the force sensor wiring on the finishing force cannot be completely eliminated and the VSFFs of media at different positions of a workpiece cannot be effectively measured, which limit the better understanding of the mechanism of VSF. In this work, a triaxial wireless force sensor (WFS) was developed and used to measure the VSFFs without the effect of force sensor wiring. A band-pass filter and the wavelet packet analysis method were used to eliminate the background noise induced by the vibrations of the finisher.

2. Experiment

2.1. Vibratory finishing machine and media

In the vibratory finishing machine, the horizontal centrifugal force and the vertical moment were generated by the eccentric block at the end of the driving motor connecting rod. The vibration energy is transmitted to the media in the finishing barrel through the connecting shaft and springs; thus, the spiral trajectory movement of the media and the workpiece occurred in the vibratory finishing barrel [2], which makes the workpiece surfaces be finished by the media in the barrel. The barrel of the vibrating machine is made of ring-shaped polyethylene and had an outer diameter of 780 mm, an inner diameter of 215 mm, and a depth of 450 mm. The barrel is connected to the motor through a connecting shaft. The motor drove the eccentric block at a speed of 1500 rpm, and the whole assembly is fixed on the base by three spiral springs (Fig. 1). Without loading, the vibration acceleration in the x-, y-, and z-direction was about 42 m/s^2, 39 m/s^2, and 95 m/s^2, respectively. A house-made wireless force sensor (WFS) is used to measure the surface finishing forces between the media and the workpiece, which will be described in details in the next section.

Three different media of SiC quadrangular abrasives with 6 mm in side length, resin triangular abrasives with 12 mm in side length, and corundum spherical abrasives with 6 mm, 12 mm, and 18 mm in diameters were used in this study, which is pictured in Fig. 2.

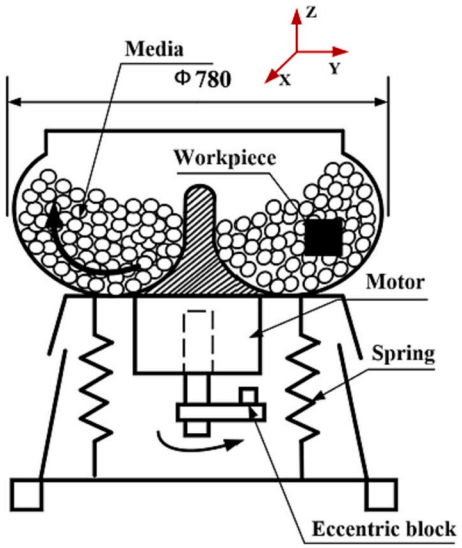

Fig. 1. Schematic diagram of the vibratory finishing machine.

2.2. Development of the wireless force sensor

The developed wireless force sensor (WFS) system consists of a triaxial force sensor (LH-SZ-40), a signal amplifier (LH-FD-DN-10 V), a data recorder (MSR160), a power supply battery (9 V), and housing, which is an independent system used to measure the VSFFs between the media and workpiece, as shown in Fig. 3. The outer case of the WFS is a rectangular aluminum alloy block with a length of 95 mm, a width of 95 mm, and a height of 90 mm. A smaller aluminum alloy cylinder with a diameter of 10 mm and length of 5 mm is fixed to the triaxial force sensor, which is interacted with the finishing media in the vibratory finisher and it can be replaced with other different materials.

The WFS has a force measurement range of ±50 N with 0–20 mV output signals that can be converted into 0–10 V signals by the signal amplifier for the data acquisition. The force measurement accuracy of the WFS is 0.5%. In the measurements, the sampling frequency of the data logger was set to 512 Hz.

2.3. Wireless force sensor calibration

2.3.1. Static calibration

Before the VSFF measurements, the static calibration of the WFS was carried out, and before that the output signal without loading was adjusted to 5.000 V (zero-balanced). The static calibration of the WFS was carried out by increasing and decreasing the standard calibrating weights in X-, Y-, and *Z*-direction, and record the corresponding output voltage in X, Y, and Z direction, respectively. Fig. 4 demonstrates the relationship between the output voltage and the loading/unloading in *Z*-direction.

It is observed from Fig. 4 that the WFS has a very good linear relationship between the load and output voltage in Z-direction and has no significant cross-effect on X- and Y-directions.

2.3.2. Dynamic calibration

In vibratory surface finishing, the WFS is in vibrating due to the vibrations of the finisher and media, which generates output signals or background noise. These noise signals must be eliminated from the measured force signals. Therefore, the background noise of the WFS should be measured before carrying out the formal VSFF measurements, which is called the dynamic calibration of the WFS.

In the dynamic calibration of the WFS, the force-sensing surface of the WFS was covered (as shown in Fig. 5) to prevent it from contacting with finishing media in the vibratory finisher, and the output signals were recorded while the finisher was in operation. Fig. 6 (a), (b), and (c) demonstrates the signals generated by the WFS itself or the background noise of the WFS in X-, Y-, and *Z*-direction, respectively.

2.4. Surface finishing force measurement

In the vibratory surface finishing force (VSFF) measurements, the WFS was put in the vibrating barrel filled with 100 kg of media. Fig. 7 demonstrates the VSFF measurements using the WFS in vibratory finishing.

Fig. 2. Media used in the experiment. (a) SiC quadrangular media; (b) resin triangular media; (c) corundum spherical media.

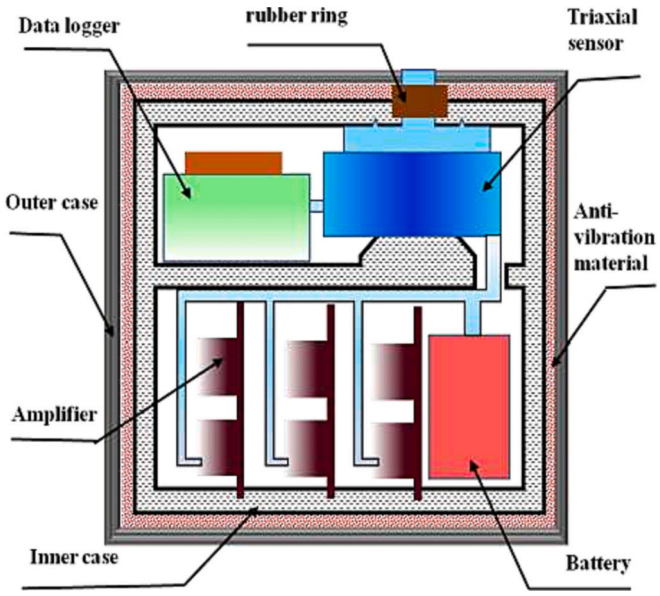

Fig. 3. Schematic diagram of the wireless force sensor.

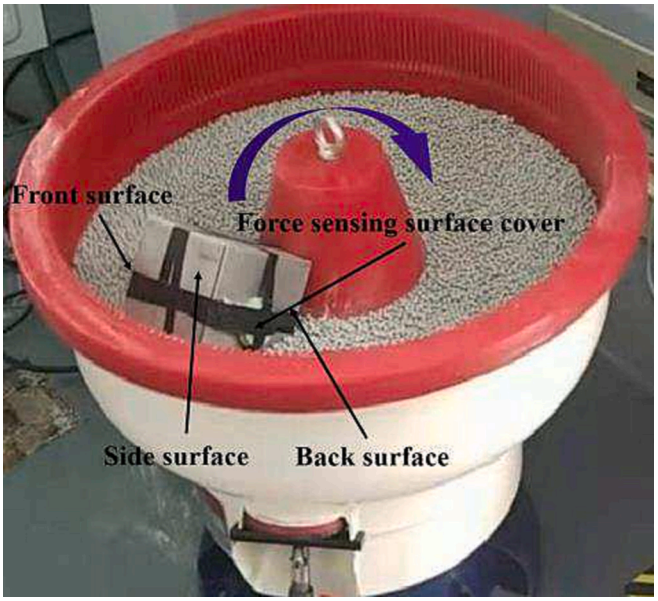

Fig. 5. Dynamic calibration of the WFS.

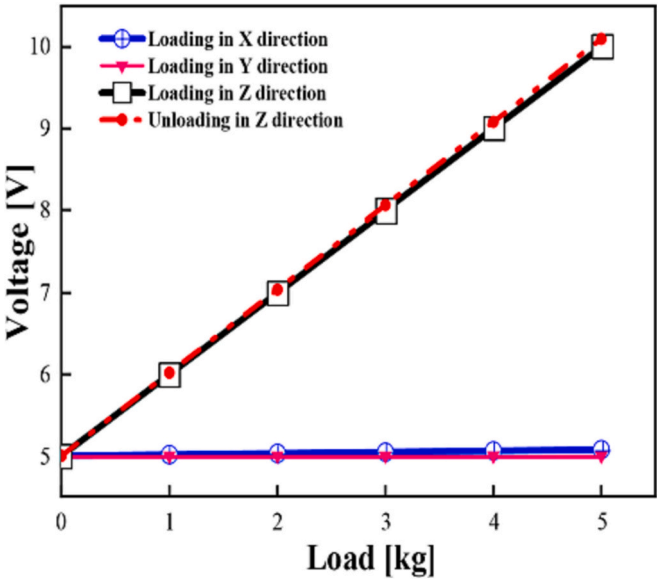

Fig. 4. Static calibration of the WFS.

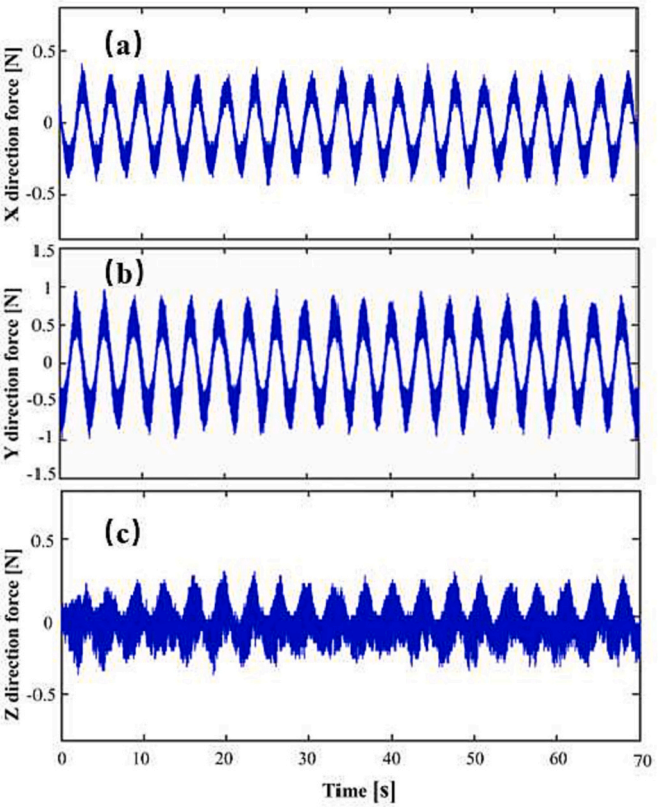

Fig. 6. Background noise of the sensor in X-, Y-, and Z-directions.

In the VSFF measurements, the WFS followed the movement of the media in the finisher. It rotated around its axis and also around the island of the finisher, generating a spiral movement. The measured force signals were exported to a computer for analysis after the completion of the measurements.

In order to compare the effectiveness of surface finishing for different surfaces of the workpiece, the VSFFs from three different surfaces of the workpiece, i.e. the front surface facing the media travel direction, the rear surface opposite to the media travel direction, and the side surface facing the island of the finisher, were measured separately.

Since the background noise is included in the measured output signals from the WFS, the background noise as shown in Fig. 6 should be removed from the measured force signals. Fig. 8 (a) presents the measured VSFFs with background noise in *Z*-direction (normal to the contact surface of the WFS); while Fig. 8 (b) shows the measured VSFFs without background noise.

3. Results and discussion

3.1. Vibratory surface finishing force

Since the data storage of the recorder in the WFS is limited, after a certain period of testing (10 min in this study), the measured data stored in the WFS (recorder) were exported to a computer. In the data processing, wavelet denoising method was employed to remove the

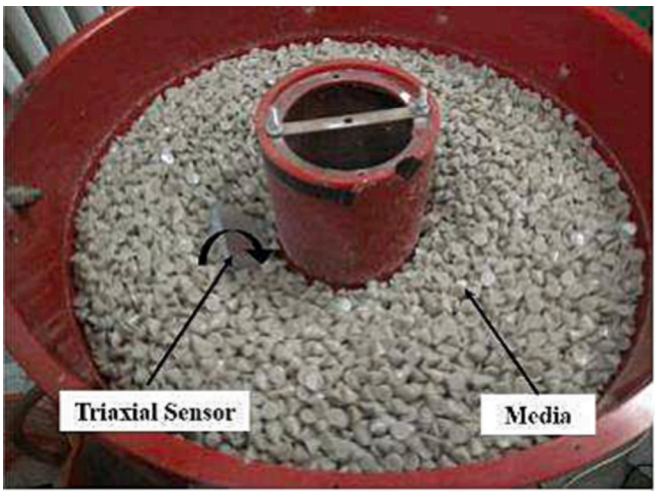

Fig. 7. VSFF measurements with the WFS.

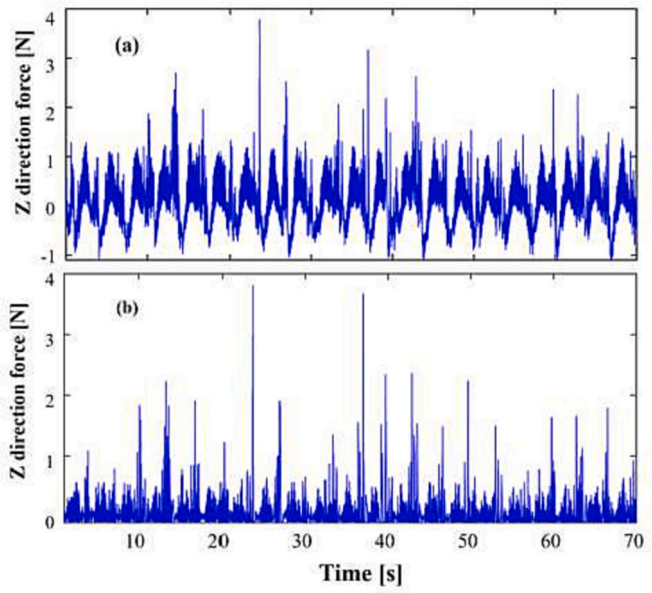

Fig. 8. Measured VSFFs in Z-direction on the side surface of the workpiece: (a) measured VSFFs with background noise; (b) measured VSFFs without background noise.

background noise using the MATLAB software. The WFS was a rectangular parallelepiped, and the VSFFs on each surface of the workpiece were measured by changing the position of the WFS in the finisher.

Fig. 9 (a), (b), and (c) demonstrates the measured VSFFs without background noise between the SiC dielectric media and the front surface of the workpiece in X-, Y-, and *Z*-direction, respectively. It is observed from Fig. 9 that the measured VSFFs in *Z*-direction are much larger than that in X- and Y-directions, indicating that the normal impacts between the media and workpiece are dominant. Therefore, in this study the effects of the workpiece surface and media on the VSFFs are focused on the Z-direction, which will be presented in the following sections.

3.2. *Effect of workpiece surface on the VSFFs*

The measured normal contact forces or the VSFFs in Z-direction between the SiC media and the front surface, side surface, and rear surface of the workpiece are presented in Fig. 10 (a), (b), and (c), respectively. Fig. 11 shows the measured VSFFs occurrences between

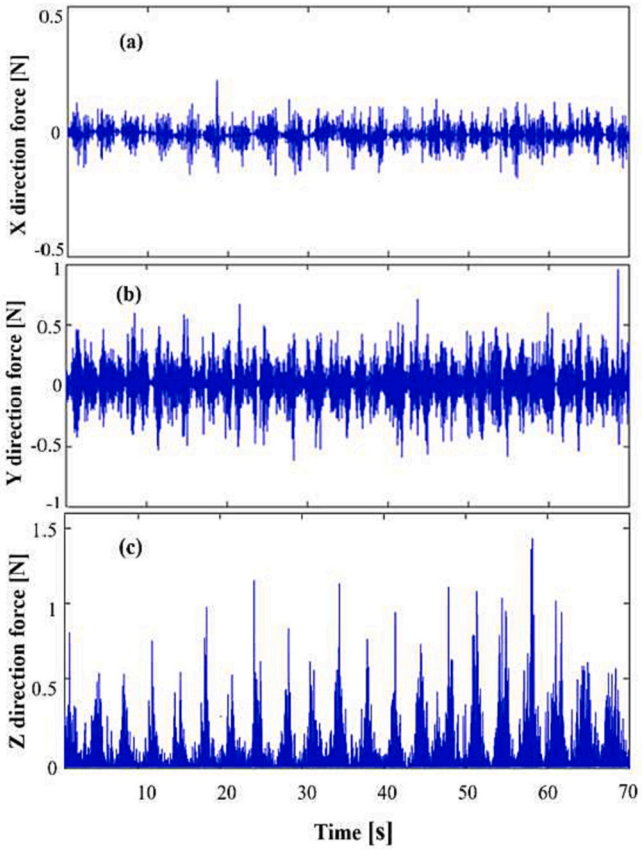

Fig. 9. Measured VSFFs between the front surface of the workpiece and SiC dielectric media: (a) X-direction, (b) Y-direction, and (c) *Z*-direction.

the SiC dielectric media and different surfaces of the workpiece; while Table 1 lists the measured mean normal contact forces (mean VSFF in Z-direction) between the SiC media and workpiece.

It is observed from Figs. 10 and 11 that the largest number of impacts with contact force larger than 0.5 N are occurred on the front surface of the workpiece, but on the rear surface the smallest number of impacts with contact force larger than 0.7 N are occurred. Table 1 lists the measured impact energy and mean normal contact force between the SiC media and workpiece without noise. It is observed that without background noise the largest impact energy and mean normal contact force occurs on the front surface of the workpiece, followed by the side and rear surfaces.

3.3. *Effect of media material on the VSFF*

The effects of three different dielectric materials on the normal contact force were studied, namely (a) SiC dielectric, (b) resin triangular pyramid dielectric, and (c) corundum spherical dielectric. Fig. 12 (a), (b) and (c) shows the normal contact forces between the front surface of the workpiece and the media (a), (b), and (c), respectively. Fig. 13 shows the measured VSFFs occurrence between the front surface of the workpiece and the three different media; while Table 2 presents the measured impact energy and RMS normal contact forces (VSFFs in *Z*-direction) between the workpiece and media.

It can be seen from Figs. 12 and 13 that the number of effective impacts of the resin triangular pyramid media on the front surface of the workpiece is significantly smaller than that of the other two media. Since the corundum spherical media is relative smaller, the number of occurrence of smaller VSFFs (less than 0.6 N) is the largest; but for the relative larger volume SiC media, the number of occurrence of larger VSFFs (larger than 0.7 N) is the largest. Table 2 shows that the average

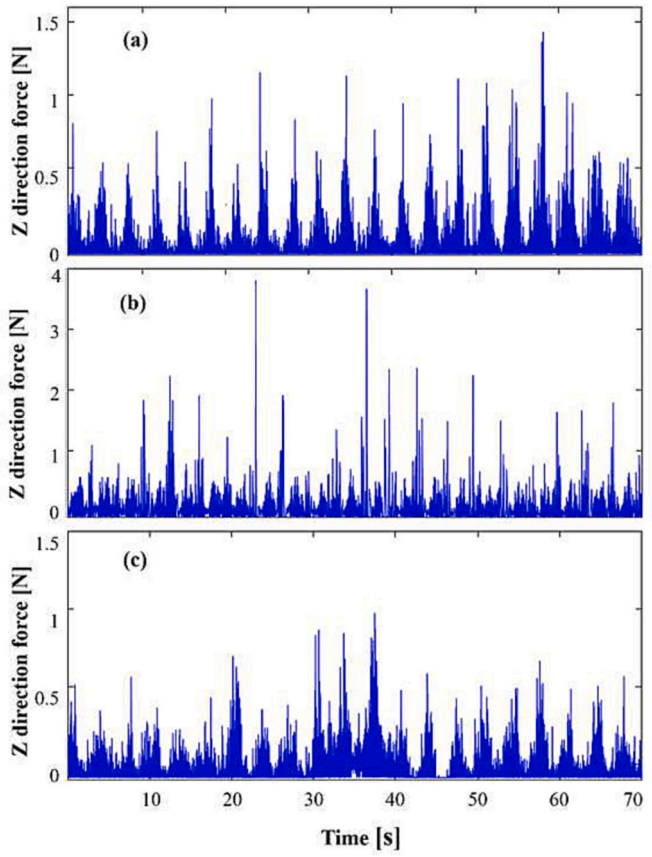

Fig. 10. Measured normal contact forces between the SiC dielectric media and the workpiece surfaces. (a) front surface; (b) side surface; (c) rear surface.

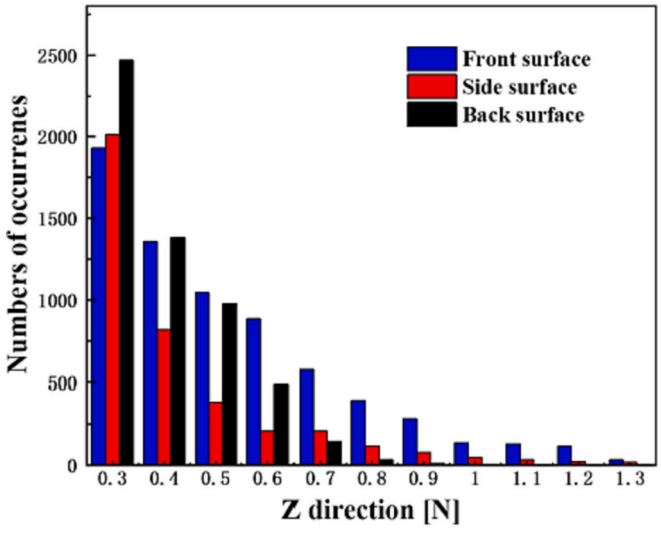

Fig. 11. Measured VSFF occurrence between the SiC quadrangular media and workpiece.

Table 1
Measured impact energy and RMS of normal contact force between the SiC quadrangular media and workpiece.

Workpiece position	Impact energy [N.s]	RMS of VSFF without noise [N]
Front surface	14.87	0.303
Side surface	10.85	0.274
Back surface	10.04	0.240

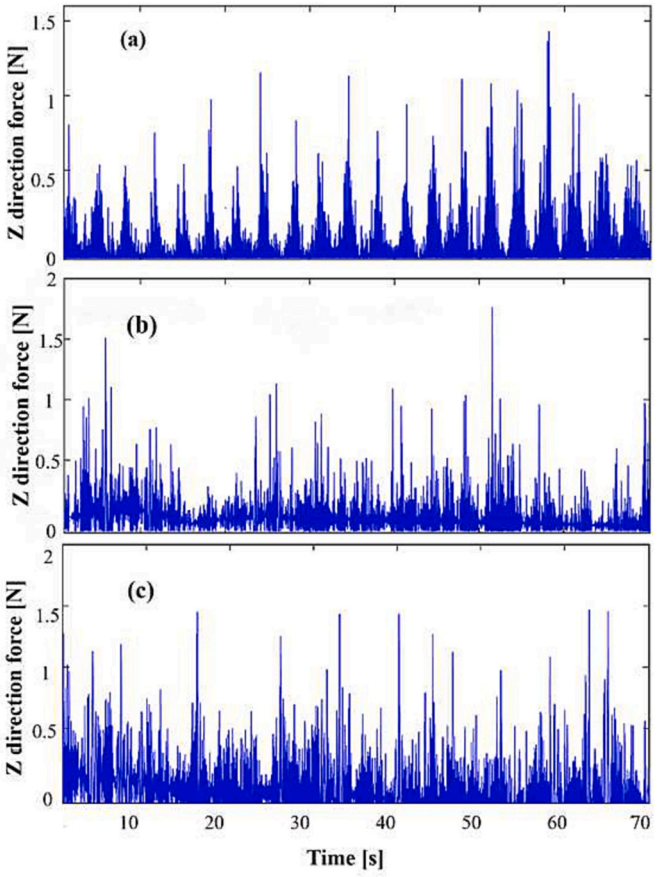

Fig. 12. Measured VSFFs in Z-direction between the front surface of workpiece and media. (a) SiC quadrangular media; (b) resin triangular media; (c) corundum spherical media.

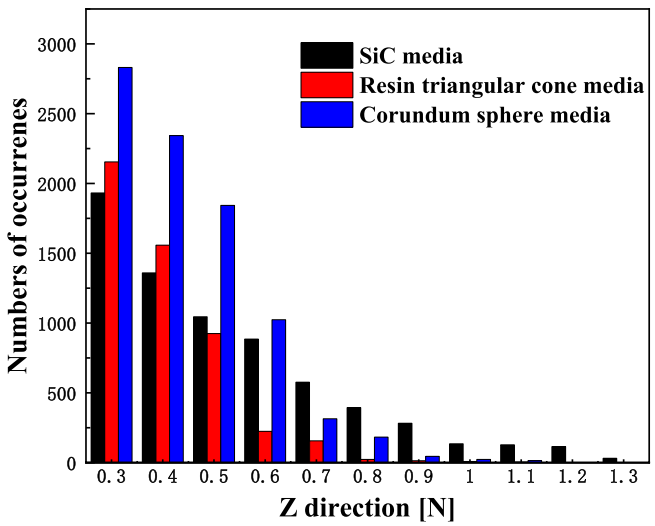

Fig. 13. Impact occurrence at the front surface of the workpiece with different media.

contact force of the resin triangular pyramid media is the largest, followed by the corundum spherical medium and the SiC quadrangular media.

Table 2
Impact energy and RMS of normal contact forces between media and the front surface of the workpiece.

Media	Impact energy [N.s]	RMS of VSFF without noise [N]
SiC quadrangular	14.870	0.303
Resin triangular	13.508	0.286
Corundum spherical	12.068	0.275

3.4. Surface roughness and hardness

3.4.1. Workpiece

In order to investigate the effects of vibratory surface finishing on the surface roughness and hardness of workpiece, four different materials of 6061 aluminum alloy (AA-6061), 7075 aviation aluminum alloy (AA-7075), A3 steel, and stainless steel were used as the workpiece materials. To save experimental time, smaller specimens (30 × 20 × 5 mm) made of the above mentioned four materials were inserted into the surface of a larger workpiece that is in the same dimension as that of the WFS described in sections 3.1–3.3. The larger workpiece was made of AA-6061 and its weight (including the smaller specimens) is similar to that of the WFS. Fig. 14 illustrates the overview of the workpiece with experimental specimens.

3.4.2. Surface roughness

After vibratory surface finishing the workpiece for a certain period of time, say 30 min, 90 min, 150 min, 210 min, 270 min, and 330 min in this study, the smaller specimens were taken out from the larger workpiece. A white light interferometer (Bruker) was employed to observe the surface topographies of the specimens.

Figs. 15 (a), (b), (c), and (d) present the surface topographies of the AA-6061, AA-7075, A3 steel, and stainless steel specimens, respectively, after vibratory surface finishing with SiC abrasive media for 0 min, 30 min, 150 min, and 330 min. Table 3 shows the roughness Ra of specimens on the front surface after vibratory finishing with SiC dielectric media. It is observed from Table 3 that the surface roughness Ra of all the four materials is reduced with the increasing of finishing time. The surface roughness of stainless steel reduced to 20% of that the original surface roughness after VSF for 330 min; while the surface roughness of the AA-6061, AA-7075, and A3 steel reduced to 53.8%, 65.9%, and 38.6% of its original surface roughness, respectively.

Fig. 16 presents topographies of AA-6061 specimens from the front, side, and rear surfaces of the workpiece, after VSF with the SiC dielectric media for 30 min, 150 min, and 330 min, respectively. Table 4 compared the efficiency of VSF with the SiC dielectric media on the surface roughness (Ra) of AA-6061 at different positions (front, side, and rear surfaces) of the workpiece. Table 4 shows that VSF has the best performance in surface roughness reduction on the front surface with 54.5% Ra reduction after VSF for 330 min operation, followed by side and rear surfaces with 43.3% and 42.2% Ra reduction, respectively.

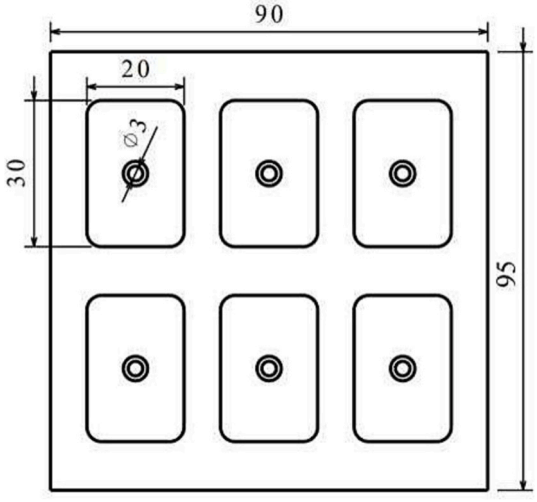

Fig. 14. Overview of the workpiece.

Fig. 17 (a) clearly shows that stainless steel has the smallest surface roughness after surface finishing for 30 min, and after surface finishing for 150 min the surface roughness of stainless steel is stable, but the surface roughness of AA-6061 and A3 steel is decreasing with surface finishing time in the whole processing period. However, the surface roughness of AA-7075 is slightly increased after surface finishing for 270 min. Fig. 17 (b) shows that after VSF, the front surface roughness of the workpiece reduced more quickly and has the smallest surface roughness followed by the side and rear surfaces, indicating that at the position of the front surface the finishing effectiveness is the highest and followed by the side and rear surfaces. With the increasing of vibratory surface finishing time, the surface finishing effectiveness at the two positions of side and rear surfaces of the workpiece is tending to be the same.

3.4.3. Surface hardness

The surface Rockwell hardness of the vibratory finished specimens were measured after 30 min, 90 min, 150 min, 210 min, 270 min, and 330 min of vibratory finishing with SiC dielectric media.

Fig. 18 presents the surface hardness at the side surfaces of the tested specimens after various surface finishing period of time. It is observed from Fig. 18 (a) that the surface hardness of AA-6061 is increased with the increasing of finishing time; while the surface hardness of AA-7075 is increased with the increasing of finishing time for 270 min, but decreased after that; the surface hardness of A3-steel is increased significantly in the first 30 min and then increased gradually; the surface hardness of stainless steel is increased with finishing time for 90 min and then decreased with finishing time, indicating that in vibratory surface finishing of stainless steel, the finishing time is better less than 210 min, as the surface hardness is close to its maximum but the surface roughness is close to its minimum.

4. Conclusions

A novel triaxial wireless force sensor has been successfully developed to measure the vibratory surface finishing forces (VSFFs) between the media and workpiece without being affected by the sensor wiring. The effects of media and workpiece position on the VSFFs have been studied, and the effectiveness of vibratory surface finishing with various materials of media and workpiece has been investigated. The following conclusions can be drawn.

(1) The normal impacts are dominant in the vibratory surface finishing. The impact energy and RMS of VSFFs in normal direction on the front surface of the workpiece are larger than that on the side and rear surfaces of the workpiece.
(2) The size or mass of media had a significant effect on the VSFFs. The peak VSFFs of larger mass media were higher than those of smaller mass media, but the impact frequency of larger media was lower than that of smaller size media.
(3) Both the VSFFs and media shapes have significant effect on the surface roughness and hardness of the workpiece.
(4) After vibratory surface finishing for 330 min, the surface roughness of Al-6061, Al-7075, A3 steel, and stainless steel reduced to 53.8%, 65.9%, 38.6%, and 20% of the original surface roughness, respectively.
(5) The surface hardness of AA-6061 and A3 steel was increased with the increasing of VSF in the whole operation period of 330 min; while the surface hardness AA-7075 and stainless steel was increased with VSF for 270 min and 210 min, respectively.

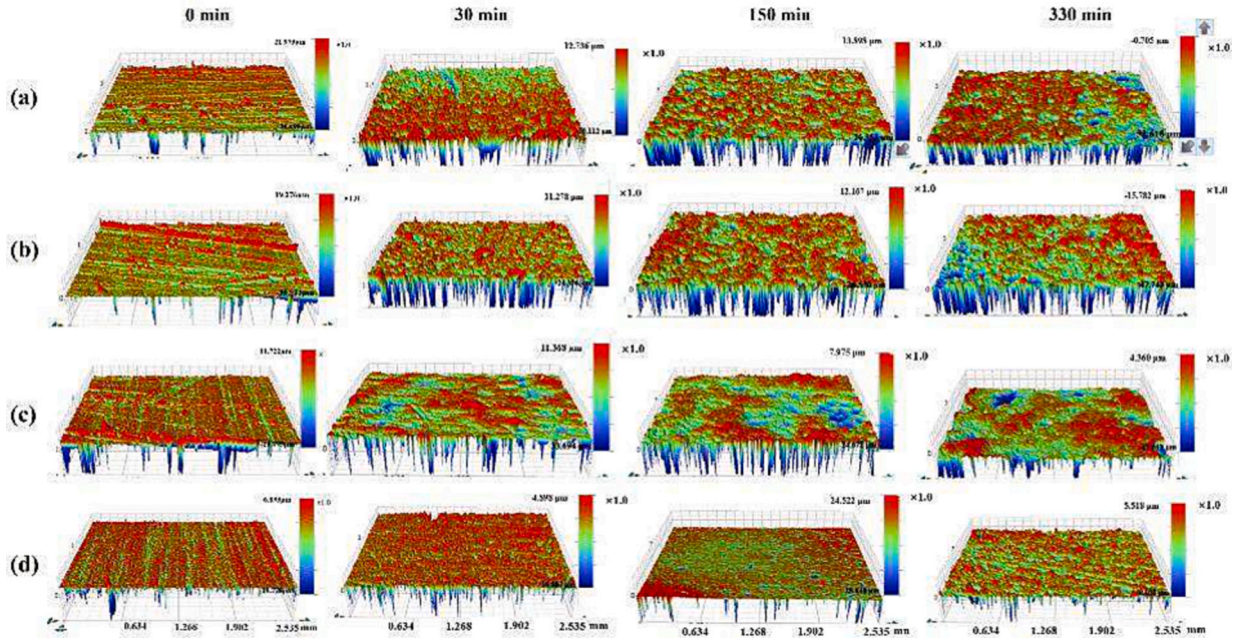

Fig. 15. Effects of SiC dielectric medium on the front surface topography of different workpiece samples after different surface finishing times. (a) AA-6061; (b) AA-7075; (c) A3 steel; (d) stainless steel.

Table 3
The roughness Ra of specimens on the front surface after vibratory finishing with SiC dielectric media.

Processing period [min]	AA-6061 [μm]	AA-7075 [μm]	A3 steel [μm]	Stainless steel [μm]
0	2.75	2.05	3.25	2.35
30	1.9	1.75	1.72	1.18
150	1.64	1.62	1.38	0.58
330	1.48	1.35	1.255	0.47
Reduced (%)	46.2%	34.1%	61.4%	80%

(6) In order to get the best surface quality of workpiece in vibratory surface finishing, the media material and shape/size, finishing period of time, initial position of the workpiece, and other operation conditions should be optimized.

CRediT authorship contribution statement

Shuwen Wang: Conceptualization, Methodology, Resources, Funding acquisition, Data curation, Validation, Supervision, Writing – review & editing. **Jiahui Chen:** Investigation, Formal analysis, Writing – original draft. **Zhiguo Liu:** Investigation, Formal analysis, Writing – original

Table 4
Effect of SiC dielectric media on surface roughness at different positions of AA-6061 workpiece after surface finishing.

Surface finishing period [min]	Front surface [μm]	Side surface [μm]	Back surface [μm]
0	2.75	2.75	2.75
30	1.65	1.94	2.3
150	1.5	1.58	1.66
330	1.25	1.56	1.59
Reduced (%)	54.5%	43.3%	42.2%

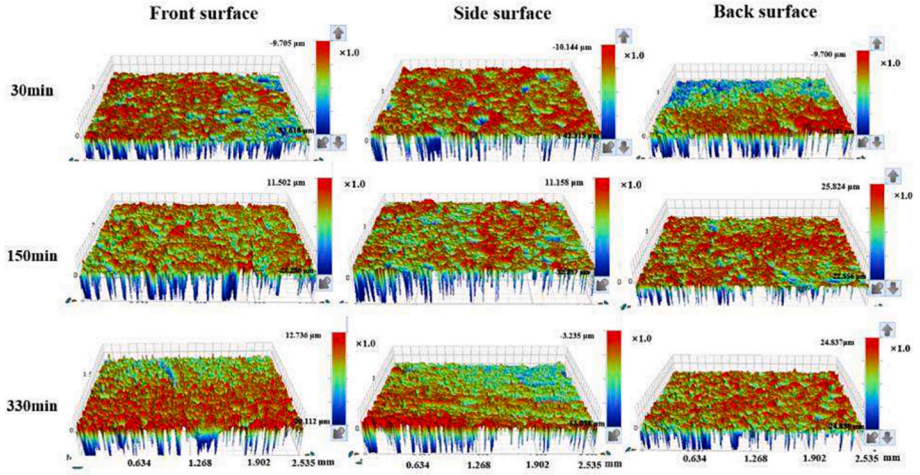

Fig. 16. Effects of SiC dielectric media on the surface topography at different positions of AA-6061 workpiece after various of finishing periods: (a) 30 min, (b) 150 min, and (c) 330 min.

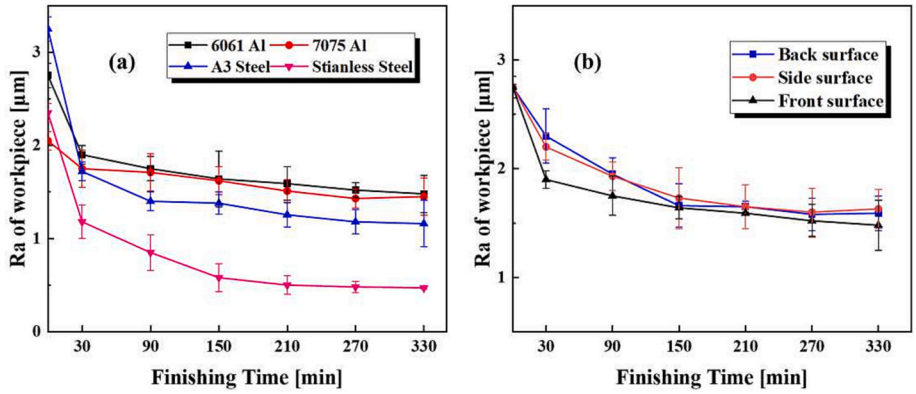

Fig. 17. Relationship between surface roughness and finishing time with SiC quadrangular media. (a) comparison of various specimen materials; (b)comparison of three surfaces on the workpiece.

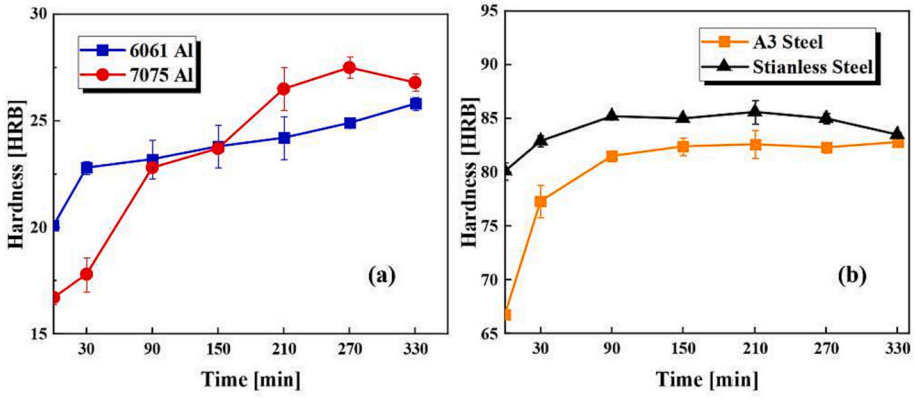

Fig. 18. Surface hardness of specimens after vibratory finishing with SiC quadrangular media.

draft. **Michael Morgan:** Resources, Funding acquisition, Validation, Supervision, Writing – review & editing. **Xiaoxiao Liu:** Investigation, Project administration, Validation, Writing – review & editing.

Declaration of Competing Interest

The authors declare that they have no known competing financial interests or personal relationships that could have appeared to influence the work reported in this paper.

Data availability

Data will be made available on request.

Acknowledgments

This work was financially supported by the Science and Technology Commission of Shanghai Municipal (Grant No.: 18060502400) and the Natural Science Foundation of Shanghai (Grant No.: 21ZR1445000); Engineering and Physical Sciences Research Council of UK (Grant No. EP/N022998/1).

References

[1] A. Rodríguez, M. González, O. Pereira, L.N. López de Lacalle, M. Esparta, Edge finishing of large turbine casings using defined multi-edge and abrasive tools in automated cells, Int. J. Adv. Manuf. Technol. (2021), https://doi.org/10.1007/s00170-021-08087-y.

[2] C. Zhang, W. Liu, S. Wang, Z. Liu, M. Michael, X. Liu, Dynamic modeling and trajectory measurement on vibratory finishing, Int. J. Adv. Manuf. Technol. 106 (2020) 253–263, https://doi.org/10.1007/s00170-019-04644-8.

[3] S. Wang, R.S. Timsit, J.K. Spelt, Experimental investigation of vibratory finishing of aluminum, Wear 243 (2000) 147–156, https://doi.org/10.1016/S0043-1648(00)00437-3.

[4] A. Chaurasia, N. Rattan, R.S. Mulik, Magnetic abrasive finishing of AZ91 magnesium alloy using electromagnet, J. Braz. Soc. Mech. Sci. Eng. 40 (2018), https://doi.org/10.1007/s40430-018-1399-7.

[5] R.S. Mulik, P.M. Pandey, Experimental investigations and modeling of finishing force and torque in ultrasonic assisted magnetic abrasive finishing, J. Manuf. Sci. Eng. Tran. ASME 134 (2012), https://doi.org/10.1115/1.4007131.

[6] A. Avilés, R. Avilés, J. Albizuri, L. Pallarés-Santasmartas, A. Rodríguez, Effect of shot-peening and low-plasticity burnishing on the high-cycle fatigue strength of DIN 34CrNiMo6 alloy steel, Int. J. Fatigue 119 (2019) 338–354, https://doi.org/10.1016/j.ijfatigue.2018.10.014.

[7] R. Avilés, J. Albizuri, A. Lamikiz, E. Ukar, A. Avilés, Influence of laser polishing on the high cycle fatigue strength of medium carbon AISI 1045 steel, Int. J. Fatigue 33 (2011) 1477–1489, https://doi.org/10.1016/j.ijfatigue.2011.06.004.

[8] E. Ukar, A. Lamikiz, S. Martínez, I. Tabernero, L.N. López de Lacalle, Roughness prediction on laser polished surfaces, J. Mater. Process. Technol. 212 (2012) 1305–1313, https://doi.org/10.1016/j.jmatprotec.2012.01.007.

[9] A. Rodríguez, L.N. López de Lacalle, A. Celaya, A. Lamikiz, J. Albizuri, Surface improvement of shafts by the deep ball-burnishing technique, Surf. Coat. Technol. 206 (2012) 2817–2824, https://doi.org/10.1016/j.surfcoat.2011.11.045.

[10] A. Yabuki, M.R. Baghbanan, J.K. Spelt, Contact forces and mechanisms in a vibratory finisher, Wear 252 (2002) 635–643, https://doi.org/10.1016/S0043-1648(02)00016-9.

[11] M.R. Baghbanan, A. Yabuki, R.S. Timsit, Tribological behavior of aluminum alloys in a vibratory finishing process, Wear 255 (2003) 1369–1379, https://doi.org/10.1016/S0043-1648(03)00124-8.

[12] D. Ciampini, M. Papini, J.K. Spelt, Impact velocity measurement of media in a vibratory finisher, J. Mater. Process. Technol. 183 (2007) 347–357.

[13] D. Ciampini, M. Papini, J.K. Spelt, Characterization of vibratory finishing using the Almen system, Wear 264 (2008) 671–678, https://doi.org/10.1016/j.wear.2007.06.002.

[14] X. Song, R. Chaudhari, F. Hashimoto, Experimental investigation of vibratory finishing process, in: ASME 2014 International Manufacturing Science and Engineering Conference, MSEC, 2014, https://doi.org/10.1115/MSEC2014-4093.

[15] L.D.S. Maciel, J.K. Spelt, Measurements of wall-media contact forces and work in a vibratory finisher, Powder Technol. 360 (2020) 911–920, https://doi.org/10.1016/j.powtec.2019.10.066.

[16] M. Lachenmaier, A. Dehmer, D. Trauth, P. Mattfeld, Influence of different input parameters on the contact conditions determing the surface integrity of workpiece in an unguided vibratory finishing process, Proc. CIRP 71 (2018) 53–58, https://doi.org/10.1016/j.procir.2018.05.022.
[17] K. Ahluwalia, R. Mediratta, S.H. Yeo, A novel approach to vibratory finishing: double vibro-polishing, Mater. Manuf. Process. 32 (2017) 998–1003, https://doi.org/10.1080/10426914.2016.1232812.
[18] B. Richard, V. Frederik, Contact forces in unguided vibratory finishing, in: ASME 2015 International Manufacturing Science and Engineering Conference, MSEC, 2015, https://doi.org/10.1115/MSEC20159220.
[19] B.J. Wong, K. Majumdar, K. Ahluwalia, S.H. Yeo, Effects of high frequency vibratory finishing of aerospace components, J. Mech. Sci. Technol. 33 (2019) 1809–1815, https://doi.org/10.1007/s12206-019-0333-y.
[20] F. Hashimoto, D.B. Debra, Modelling and optimization of vibratory finishing process, Cirp. Ann-Manuf. Techn. 45 (1996) 303–306, https://doi.org/10.1016/S0007-8506(07)63068-6.
[21] S. Gaggar, D. Vasudevan, P. Kumar, Application of smoothed particle hydrodynamics for the simulation and analysis of vibratory finishing process, Int. J. Adv. Manuf. Technol. 108 (2020) 183–190, https://doi.org/10.1007/s00170-020-05307-9.
[22] Y.S. Kang, F. Hashimoto, S.P. Johnson, Discrete element modeling of 3D media motion in vibratory finishing process, Cirp. Ann-Manuf. Techn. 66 (2017) 313–316, https://doi.org/10.1016/j.cirp.2017.04.092.
[23] R.Y. Yang, R.P. Zou, A.B. Yu, Microdynamic analysis of particle flow in a horizontal rotating drum, Powder Technol. 130 (2003) 138–146, https://doi.org/10.1016/S0032-5910(02)00257-7.
[24] D.J. Parker, A.E. Dijkstra, T.W. Martin, Positron emission particle tracking studies of spherical particle motion in rotating drums, Chem. Eng. Sci. 52 (1996) 2011–2022, https://doi.org/10.1016/S0009-2509(97)00030-4.
[25] N. Wang, T.T. Zhang, S.Q. Yang, Experiment and simulation analysis on the mechanism of the spindle barrel finishing, Int. J. Adv. Manuf. Technol. 109 (2020) 57–74, https://doi.org/10.1007/s00170-020-05609-y.
[26] L.D.S. Maciel, J.K. Spelt, Comparison of DEM predictions and measured wall-media contact forces and work in a vibratory finisher, Powder Technol. 366 (2020) 434–447, https://doi.org/10.1016/j.powtec.2020.02.014.
[27] K. Hashemnia, S. Pourandi, Study the effect of vibration frequency and amplitude on the quality of fluidization of a vibrated granular flow using discrete element method, Powder Technol. 327 (2018) 335–345, https://doi.org/10.1016/j.powtec.2017.12.097.
[28] W.H. Li, Z. Li, X.H. Li, Theoretical and simulation analysis of abrasive particles in centrifugal barrel finishing: kinematics mechanism and distribution characteristics, Powder Technol. 318 (2017) 518–527, https://doi.org/10.1016/j.powtec.2017.06.033.
[29] X.H. Li, W.H. Li, S.Q. Yang, Z.M. Hao, Study on polyurethane media for mass finishing process: dynamic characteristics and performance, Int. J. Mech. Sci. 138-139 (2018) 138–139, https://doi.org/10.1016/j.ijmecsci.2018.02.017.